

Supporting Information

Twisted Perylene Dyes Enable Highly Fluorescent and Photostable Nanoparticles

Tian, Zhiyuan; Shaller, Andrew D.; Li, Alexander D. Q.

Materials and Methods.

General. Solvents and reagents were purified where necessary using literature methods. ^1H - and ^{13}C -NMR spectra were recorded with a Mercury 300 (300 MHz) spectrometer in CDCl_3 . TMS was used as a reference for ^1H -NMR; 77.23ppm was adopted as the central line of CDCl_3 for ^{13}C -NMR. Reactions were monitored by thin-layer chromatography (TLC) on a precoated plate of silica gel 60 F_{254} (EM Science). Column chromatography was performed on silica gel 60 (230-400 mesh, EM Science) or flash silica gel, 32-60um (Dynamic Adsorbents). Cover glasses (Gold Seal No. 1) were purchased from Fisher. All compounds for monomer and nanoparticle synthesis were purchased from Sigma-Aldrich.

Monomer Synthesis. N-(2-(2-(2-(2-benzoyloxyethoxy)ethoxy)ethoxy)ethyl), N'-(2-(2-(2-(2-acryloyloxyethoxy)ethoxy)ethoxy)ethyl) - 1,6,7,12 - tetrachloro - 3,4,9,10 perylene-tetracarboxylic diimide (1). N-(2-(2-(2-(2-benzoyloxyethoxy)ethoxy)ethoxy)ethyl), N'-(2-(2-(2-(2-hydroxyethoxy)ethoxy)ethoxy)ethyl) - 1,6,7,12-tetrachloro - 3,4,9,10-perylenetetracarboxylic diimide was prepared following a previous literature method.⁹ The monobenzoyleated diimide (188mg, 0.19mmol) was dissolved in dry DCM (10ml) and 0.11ml triethylamine was added by syringe. Acryloyl chloride (0.02ml, 0.25mmol) was added by syringe and the reaction progress monitored by TLC (DCM/MeOH 15:1). Within 1 hour, the starting material ($R_f = 0.4$) was almost completely functionalized to the reactive monomer ($R_f = 0.6$). The reaction was quenched with MeOH and the solvent removed under reduced pressure. The mixture was subject to a silica gel column (DCM/MeOH 15:1) and the fractions containing the mono-functional monomer were combined to yield 0.189g (95% yield) which was characterized and stored at -20C prior to polymerizing. ^1H -NMR (300MHz, CDCl_3): 8.681 (s, 4H, perylene), 7.99 (d, 2H, $J=8.1\text{Hz}$, Benzoyl), 7.52 (t, 1H, $J=7.5\text{Hz}$), 7.39 (t, 2H, $J=7.5\text{Hz}$), 6.41 (dd, 1H, $^3J=17.4\text{Hz}$, $^2J=1.8\text{Hz}$, acryloyl), 6.14 (dd, 1H, $^3J=10.5\text{Hz}$, $^3J=17.4\text{Hz}$, acryloyl), 5.83 (dd, 1H, $^3J=10.5\text{Hz}$, $^2J=1.8\text{Hz}$, acryloyl), 4.47 (m, 4H, $\text{CH}_2\text{CH}_2\text{N}$), 4.43 (t, 2H, $J=4.8\text{Hz}$, CH_2 -benzoyl), 4.29 (t, 2H, $J=4.8\text{Hz}$, CH_2 -acryloyl), 3.854 (m, 4H, $\text{CH}_2\text{CH}_2\text{N}$), 3.79 (t, 2H, $J=5.1\text{Hz}$, CH_2CH_2 -benzoyl), 3.73-3.63 (m, 18H, $\text{OCH}_2\text{CH}_2\text{O}$, CH_2CH_2 -acryloyl). ^{13}C -NMR (CDCl_3): 166.550, 166.255, 162.391, 135.477, 133.071, 131.539, 131.176, 130.132, 129.731, 128.743, 128.403, 123.432, 123.280, 70.821, 70.770, 70.729, 70.302, 70.273, 69.316, 69.238, 67.933, 64.219, 63.804, 39.731.

Nanoparticle synthesis. We followed the procedure in reference 10c with a minor modification by replacing NIPAM with Acrylamide and SP with PDI.

Diameter characterization. Dynamic light scattering (DLS) measurements were carried out on a Beckman-Coulter N4 instrument at fixed scattering angles of 62.6° and 90° with the 632.8 line of a He-Ne laser as excitation source; standard polystyrene microspheres were used for instrument calibration. The average particle sizes and size distributions were obtained from the autocorrelation decay functions by CONTIN analysis using standard software package supplied by Beckman-Coulter. A JEOL 1010 transmission electron microscope (TEM) operated at 100 kV was employed to obtain TEM images. The microscope sample was prepared by placing a drop of the polymer dispersion on a carbon-coated Cu grid, followed by solvent evaporation at room temperature.

Sample preparation. Cover glasses were cleaned by soaking in a steril base bath (IPA/KOH solution) for 3-4 hours and thoroughly rinsed with 18M Ω water, followed by drying under a stream of dry nitrogen and stored in a dust-free container. Dilutions of stock nanoparticle solutions were made with milipore water. 2-5 drops of diluted solution ($\sim 0.001\text{OD}$) were spin-coated (4000RPM) onto clean cover glasses.

Microscope set up. Cover glass samples were placed on a custom-built stage of an inverted microscope (Zeiss Axiovert 200) equipped with an oil immersion objective (Zeiss, 100X, 1.3 NA) and an X-Y

nanopositioner stage (Mad City Labs). Connected to the side port of the microscope was a spectrometer (Acton Research Corp.) coupled to a liquid nitrogen cooled CCD detector (Princeton Instruments, Roper Scientific). The spectrometer was equipped with both a mirror for imaging and a grating for spectroscopy. An avalanche photo diode (APD) was used to collect photons from the bottom microscope port. Excitation light from an argon ion laser (488nm, 15mW) was directed through the back port of the microscope and redirected by an appropriate filter cube (Zeiss, filter set 16, ex485/20; bs510; em515) into the back aperture of the objective. Emission light was collected through the same objective and directed to the side or bottom port of the microscope.

Single molecule/particle imaging and spectroscopy.

Wide field imaging: A collimated laser beam was first attenuated with neutral density filters, then defocused with a lens before entering the back aperture of the microscope objective to produce wide field illumination. The image was detected by CCD, with a 2 sec dwell (integration) time per frame. Laser power was $\sim 150 \text{ W/cm}^2$ over a $40\mu\text{m}$ diameter circle at the cover glass surface.

Diffraction limited imaging: The collimated laser beam was first attenuated, then expanded to slightly overfill the back aperture of the objective with parallel rays in order to achieve a diffraction limited spot. Laser power used for diffraction limited analysis was $\sim 450 \text{ W/cm}^2$ at the cover glass surface. The sample was scanned over the laser spot using the nano-positioner and a scan area of $10 \times 10 \mu\text{m}$. Step size and dwell time for each pixel was 200 nm and 50 ms, respectively. Emission from this type of scan was directed to the bottom microscope port and onto the APD. The resulting image was analyzed statistically or used to position the laser on a specific molecule for time trace analysis or spectral acquisition. The entire scanning, image generation, and time trace routines were achieved using custom LabVIEW software.

Diffraction limited time-trace: The emission from a single molecule or particle was collected continuously by APD in 20 ms bins.

Spectral acquisition: The grating in the spectrometer was used to spectrally disperse emission from a single molecule or particle across the CCD chip. Spectra were acquired through WinSpec/32 software using a dwell time of 2 seconds.

Brightness determination: Brightness using CCD wide-field images were performed by using the nano-positioner to move a focused slide to a previously non-illuminated location with the shutter closed, opening the shutter, and collecting the first full 2-second illuminated image. All particles in the $40\mu\text{m}$ diameter illuminated spot with brightness above background were included in the statistical analysis. Brightness from diffraction-limited images was determined by moving a focused slide to a previously non-illuminated location prior to raster scanning. All particles above background within the $10 \times 10 \mu\text{m}^2$ were included in the statistical analysis. Brightness by diffraction-limited time-trace was determined for representative single-particles that had only previously been illuminated briefly during raster scanning.

Ensemble Spectra. Samples for ensemble measurements were diluted using milipore water and measured in standard 1 cm quartz cuvettes. Fluorescence spectra were recorded with a SPEX Fluorolog-3-21 spectrofluorometer with excitation at 488 nm. UV-vis spectra were recorded with a Varian Cary 100 spectrophotometer. For QY determination, ABS was less than 0.1; rhodamine 6G was used as a reference (QY = 0.95, λ_{EX} = 488 nm in EtOH).

Table S1. Reported nanoparticle brightness summary.

Ref ¹	Dia ² (nm)	Stated brightness (SM eq.) ³	How Meas. ⁴	NP Type ⁵	Remarks
6a	60	10 ⁴	Calc.	Silica	
6b	70	1290	Calc.	Silica	
6c	10	50	Calc.	poly core silica shell	
6d	40- 600	100	Calc.	core-shell Silica	
6e	20	10 ³ ~10 ⁴	Calc.	Polymer	1)Two-photon excitation 2)SP time-trace only 20-30 x brighter
1c, 2b	4.2	20	SP Expt.	Core-shell QD	Calibrated to commercially stated NP brightness
7a	44	<20	SP Expt.	Polymer	
7b	20	20	SP Expt.	streptavidin coated QD	
7c	20	<10	SP Expt.	Polymer	
7d, 5h	30	20	SP Expt.	Core-shell Silica	
7e	10, 40	-	SP Expt.	Quantum rod	Reported twice as bright as QD with unknown brightness and 9% QY
1L	92	4000	SP Expt.	QD-polymer nanobead	TEM shows possible aggregates
-	100	7400	Not Report	Latex Bead	Commercial latex bead, ⁶ We measured as ~250 times brighter than SM

¹ Reference number from the main text

² As determined by TEM.

³ Brightness in single molecule equivalents such as rhodamine 6G.

⁴ Calculated or single-particle experiment. Calculating single-particle brightness from ensemble measurements, either by extrapolating ensemble brightness to a single particle or multiplying ensemble Φ_n by the number of fluorophores per particle probably overestimates typical particle brightness because:

- a) Ensemble illumination power is relatively low. Only a small % of fluorophores in each nanoparticle are excited at any given time, greatly reducing effects such as singlet-singlet annihilation which decrease quantum yield during single particle imaging;
- b) There may be a large error in estimating the number of dyes per particle;
- c) There may be a large error in estimating the nanoparticle concentration;
- d) It is difficult to accurately measure the extinction coefficient for fluorophores embedded in nanoparticle colloids because of light scattering (Tyndall effect);
- e) Possible inner-filter effects.

⁵ Polymer, Silica, or quantum-dot (QD). Core-shell structures are noted.

⁶ A commercially available FNP, with $\lambda_{\text{abs,max}} = 488\text{nm}$ and reported diameter of 100nm, was used as a reference to evaluate the relative brightness of our FNPs. Accounting for the reported diameter and optimal excitation wavelength, our FNPs sample is about 5.8 times brighter than the commercial sample. DLS measured a hydrodynamic radius for the commercial sample of 185nm.

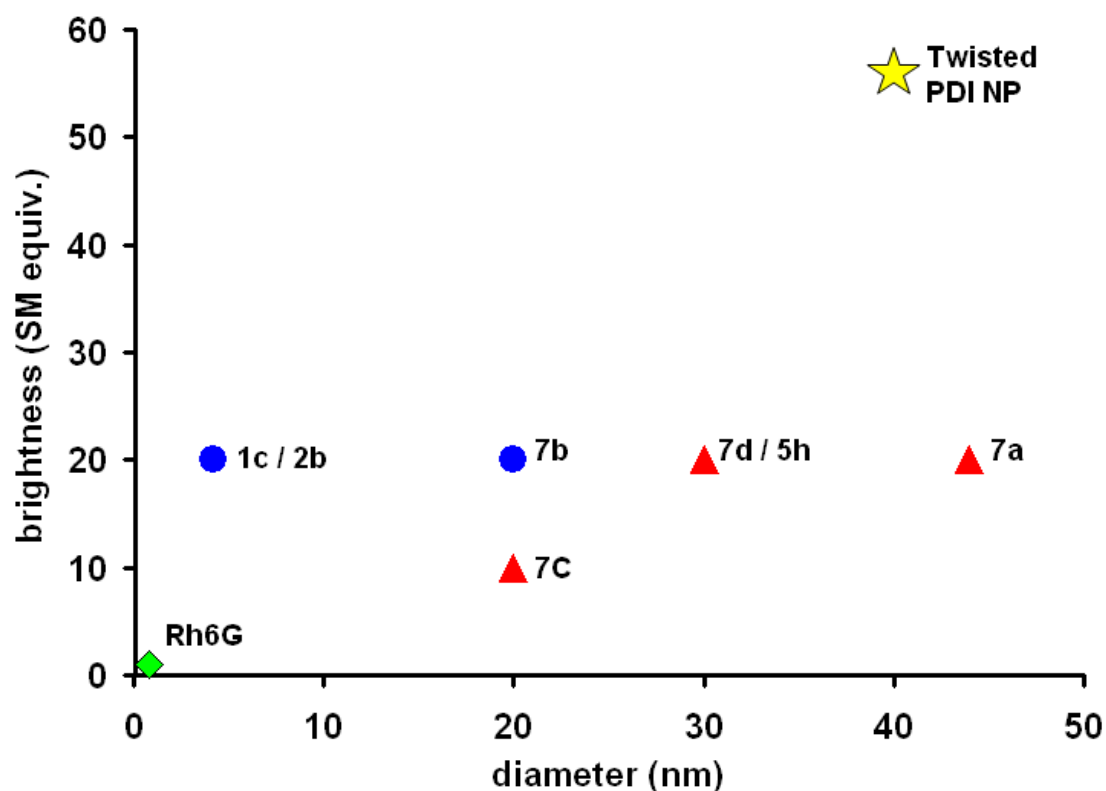


Figure S1. Brightness vs. diameter for selected nanoparticles from table S1. Only particles with diameter < 50nm and brightness determined by single particle experiments are shown. The twisted PDI nanoparticles (★) are considerably brighter than previously reported quantum dot (●) and polymer particles (▲). Brightness is reported in single molecule equivalents such as rhodamine 6G (◆). References from the main text are listed to the right of each data point.

Table S2. Compare Cl₄ PDI nanoparticle to monomer brightness by detection method.

Technique	Method	Excitation Power	Integration Time	Brightness compared to a single monomer				
				Monomer	0.3%	0.6%	1.2%	2.4%
Single Molecule	CCD image	150 W/cm ²	2 sec	1	7	19	25	56
	APD image	450 W/cm ²	50 msec / pixel	1	19	32	43	78
	APD time trace (t=0)	450 W/cm ²	20 msec	1	30	80	110	220
	APD time trace (t=400s)	450 W/cm ²	20 msec	0	9	17	36	51
Ensemble	Φ_{fl}			0.9	0.5	0.5	0.3	0.2

Nanoparticle compared to monomer brightness as measured by three methods. CCD and APD images provide average population values. APD time-traces are for single representative particles at each concentration (Figure 3, main text). Brightness determined by APD images and initial time trace are relatively higher than determined by CCD because few emitters have photobleached during the short illumination. The brightness compared to the monomer scales approximately linearly with increasing fluorophore concentration. The measured ensemble quantum yield is also provided for comparison.

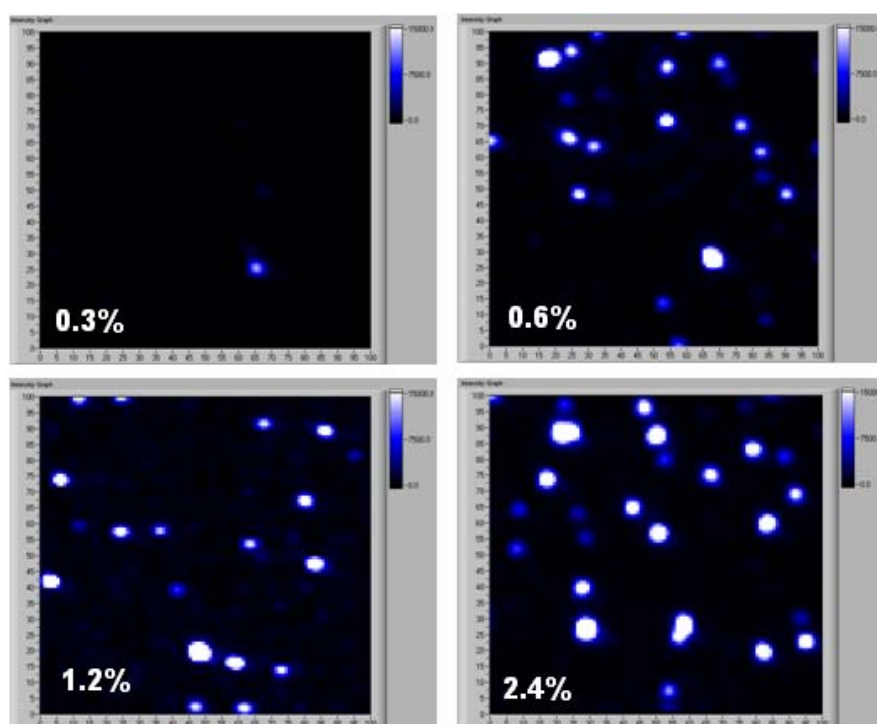


Figure S2. Four example “APD images” created by raster-scanning the sample over the diffraction-limited laser spot. Each scan is 10-μm x 10-μm and the scale is set from 0 (black) to 15000 (white). While there are some spots with >1 particle within the diffraction-limited focus, there is an obvious increase in brightness for the average particles with increasing concentration.

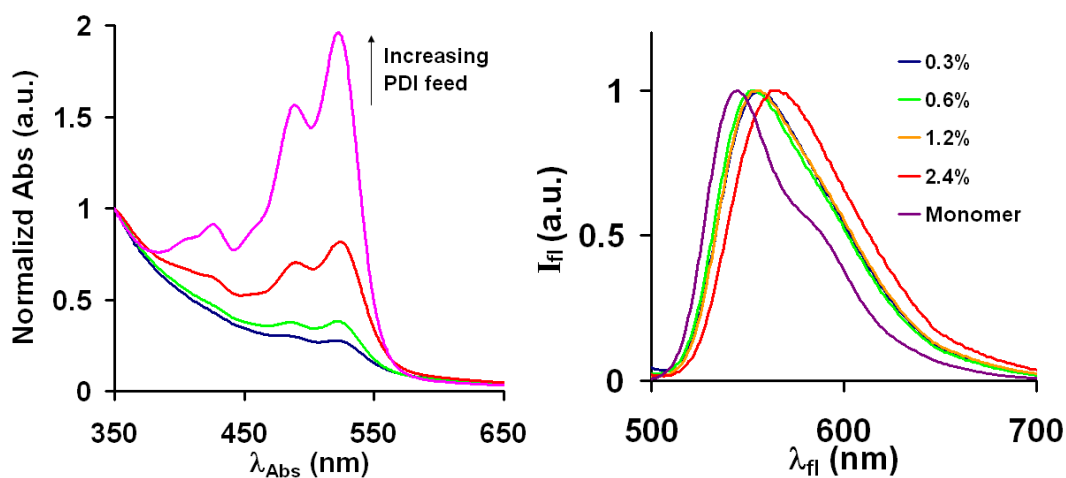


Figure S3. a) Ensemble absorbance spectra of nanoparticle solutions normalized to abs_{350} . As the % dye added is increased, its absorbance increases compared to the nanoparticle scattering. b) Ensemble fluorescent spectra of the various nanoparticle solutions (aq) compared to the monomer (CH_2Cl_2). The spectra for the 0.3, 0.6, and 1.2 w/w % samples are nearly identical while the 2.4% sample is slightly bathochromatically shifted from the other samples.

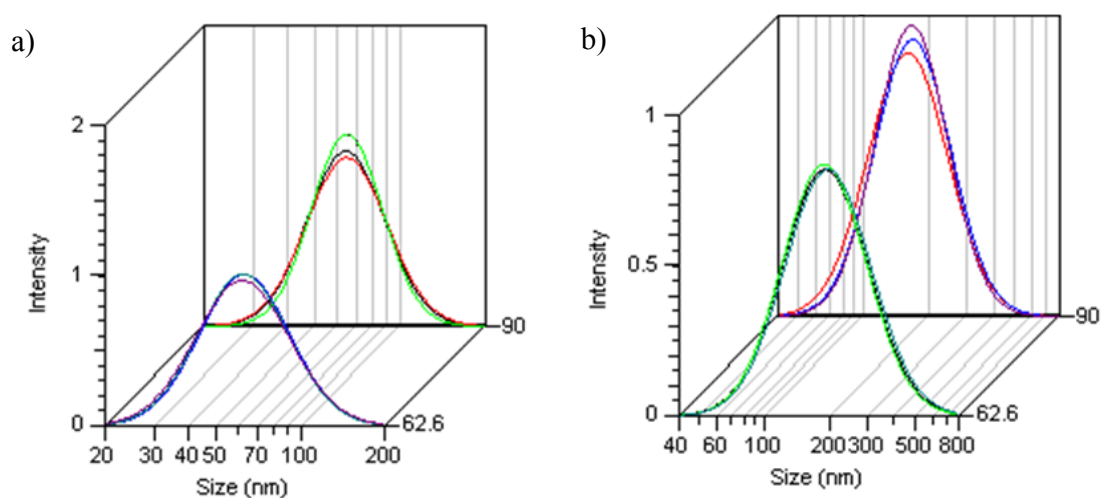


Figure S4. a) Dynamic light scattering (DLS) reports spherical particles an average *hydrodynamic* radius of 65nm for all of our samples (0.6 w/w % batch shown here). The discrepancy with the average *dry* particle size reported by TEM (40 nm) has been discussed elsewhere.^{10c} b) Similarly, DLS for a commercial fluorescent latex nanoparticle with reported diameter of 100 nm exhibits a *hydrodynamic* radius of ~185 nm, evidence of similar hydrodynamic swelling.

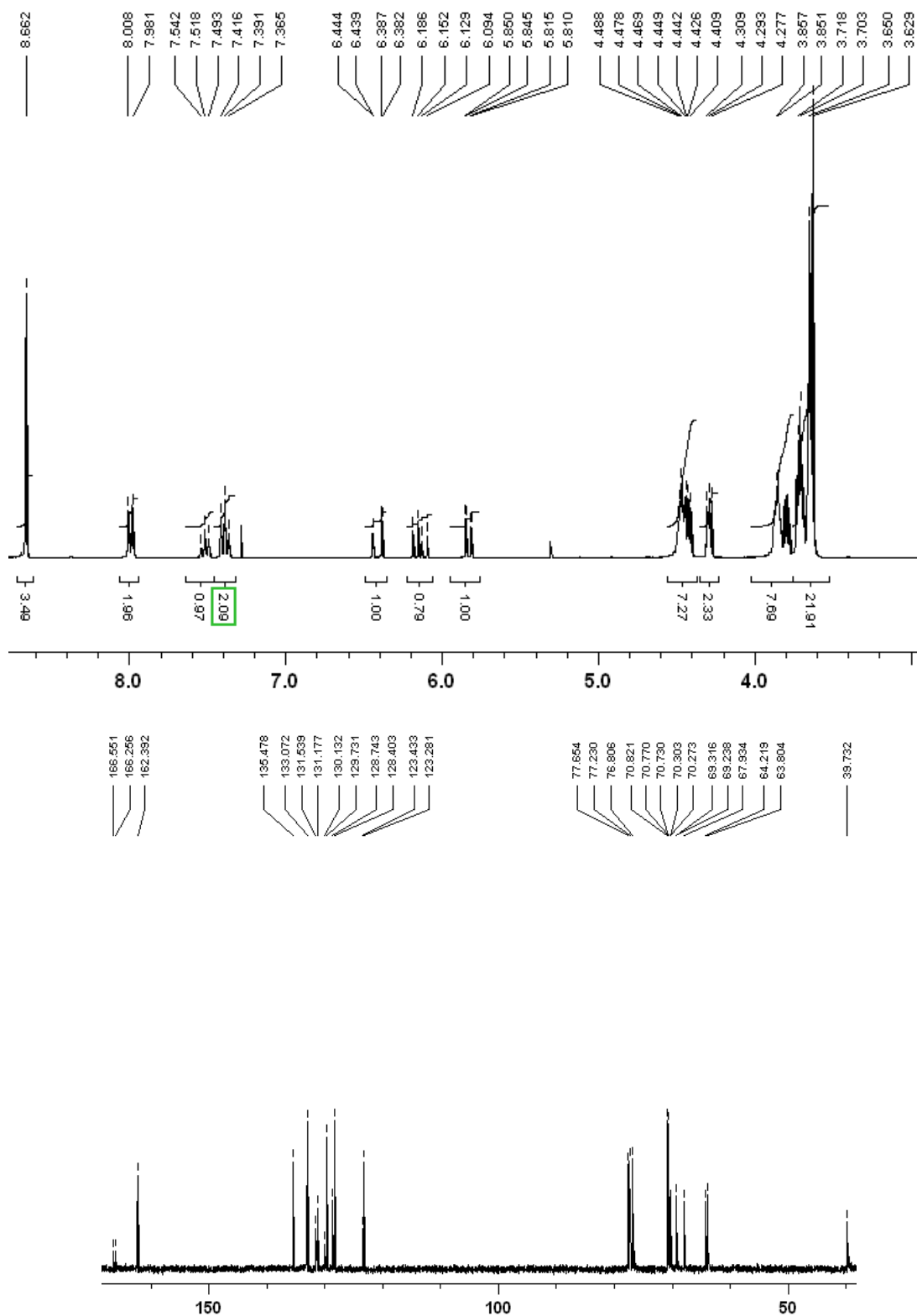


Figure S5. a) ¹H-NMR and b) ¹³C-NMR spectra for compound 1.